Vol 17 No 5, May 2008
1674-1056/2008/17(05)/1709-07

Chinese Physics B

© 2008 Chin. Phys. Soc.
and IOP Publishing Ltd

A dynamic macromodel for distributed parameter magnetic microactuators*

Fang Yu-Ming(方玉明)[a)b)†], Huang Qing-An(黄庆安)[a)], and Li Wei-Hua(李伟华)[a)]

[a)] *Key Laboratory of MEMS of Ministry of Education, Southeast University, Nanjing* 210096, *China*

[b)] *Department of Optoelectrical Engineering, Nanjing University of Posts and Telecommunications, Nanjing* 210003, *China*

(Received 17 June 2007; revised manuscript received 25 September 2007)

This paper presents a reduced-order model to describe the mechanical behaviour of microbeam-based magnetic devices. The integration for magnetic force is calculated by dividing the microbeam into several segments, and the nonlinear equation set has been developed based on the magnetic circuit principle. In comparison with previous models, the present macromodel accounts for both the micro-magnetic-core reluctance and the coupling between the beam deflection and magnetic force. This macromodel is validated by comparing with the experimental results available in some papers and finite-element solutions.

Keywords: magnetic microactuator, macromodel, microelectromechanical systems (MEMS)
PACC: 0710C, 7270, 7220F, 0670M

1. Introduction

Recently, much interest has been attracted to magnetic microactuators.[1−8] Compared to electrostatic microactuators, the electromagnetic actuators can be typically operated at substantially smaller voltages but might require larger driving currents. The electromagnetic microactuators offer distinct advantages in strength, polarity and distance of actuation. Designers of such microactuators need efficient and accurate analysis models to investigate design alternatives. However there are only a few simple analysis models[1,3,5] for electromagnetic microactuators. The previous models are often insufficient to reveal details of device operation and critical technological issues as compared with many efficient and accurate electrostatic actuator models,[9−17] although there is a similarity between the electric and the magnetic domains. Tilmans[10] presented an electromagnetic actuator small-signal dynamic model based on using the linear mode shapes of a microstructure as basis functions, which neglect the reluctance of magnetic core; thus this model is only appropriate in macro-scale. In the conventional macro-scale case, the reluctance of the magnetic core is usually negligibly small compared with that of the gap. Most of the magnetic energy is stored in the gap. But in a magnetic microactuator, the reluctance of the magnetic core has a comparable value to or even exceeds the gap reluctance due to the fabrication limitations.[1,3] The total energy stored in the system is the sum of the energy stored both in the core and the gap. Ahn and Allen[1] presented a simple lumped-parameter model accounting for the micro-magnetic core reluctance for the magnetic microactuator. But his model was based on neglecting the coupling between the magnetic force and the structure deformation. Nami *et al*[3] proposed a coupling model for magnetic microactuator to account for the micro-magnetic core reluctance via an energy-based criterion, which is a lumped parameter model and is valid only for very small deformations.

The aim of the present paper is to present a reduced-order model to describe the mechanical behaviour of distributed-parameter microbeam-based magnetic devices. In comparison with previous models, the present model can account for the micro-magnetic-core reluctance and the coupling between the beam deflection and magnetic force. Furthermore, it is validated by comparing with experimental results available in Ref.[1] and finite-element solutions. The rest of the paper is organized as follows. Section 2 describes the reduced-order model for microbeam-based magnetic devices. Section 3 calculates the static de-

*Project supported in part by the National High Technology Research and Development Program of China (Grant No 2006AA04z302).
†E-mail: fangym@njupt.edu.cn

flection of microbeam due to a magnetic force induced by the dc polarization current, and compares the results with the experimental results available in Ref.[1] and finite-element solutions. Finally, a conclusion is given in Section 4.

2. Mechanic-magnetic coupling model for microactuators

A magnetic microactuator[1] shown in Fig.1 serves as an example in this paper. The actuator works as follows. A current through the conductor coils causes flux to generate in the core. The windings of the coils are such that the flux as generated in both halves of the actuator will add in the centre part. In the centre part of the actuator, a cantilever beam of magnetic material is suspended over a base plate also of magnetic material. The flux is thus forced through the air gap between the cantilever beam and the lower magnetic contact. A force of magnetic origin is thereby created that acts to reduce the total reluctance of the magnetic circuit by attracting the released cantilever beam toward the bottom magnetic contact. Figure 2 is a schematic diagram for the magnetic microactuator, where L is the length of cantilever beam, $L_{\rm ol}$ is the overlap length, g is the gap separation, and $l_{\rm core}$ is the total length of the magnetic core. The magnetic load applied to the microbeam is composed of a dc polarization current I_0 and an ac component $i(t)$ designed to excite harmonic motions. The total current is $I_{\rm A} = I_0 + i(t)$, and $i(t) \ll I_0$. The equation of motion that governs the transverse deflection $y(x,t)$ is written as

$$\rho bh\frac{\partial^2 y(x,t)}{\partial t^2} + c\frac{\partial y(x,t)}{\partial t} + EI\frac{\partial^4 y(x,t)}{\partial x^4} = f(x, y(x,t), t), \tag{1}$$

where E is Young's modulus, I is the moment of inertia of the cross section, t is time, c is the viscous parameter, $f(x, y(x,t), t)$ is the magnetic force, ρ denotes the specific mass of the microbeam, b and h are the width and thickness of the microbeam, respectively. The microbeam deflection $y(x,t)$ is composed of a static component due to the dc current I_0, denoted by $Y_0(x)$, and a small dynamic component due to the ac current $i(t)$, denoted by $\hat{y}(x,t)$; that is

$$y(x,t) = Y_0(x) + \hat{y}(x,t). \tag{2}$$

Using modal analysis techniques,[18] $\hat{y}(x,t)$ can be expressed as

$$\hat{y}(x,t) = \sum_{m=1}^{N} \phi_m(x) q_m(t), \tag{3}$$

where $\phi_m(x)$ are the mth linear undamped mode shape of the microbeam at $Y_0(x)$, and $q_m(t)$ are the generalized coordinates.

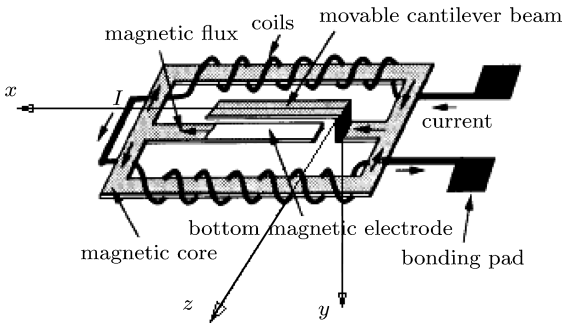


Fig.1. An example of a magnetic microactuator in Ref.[1].

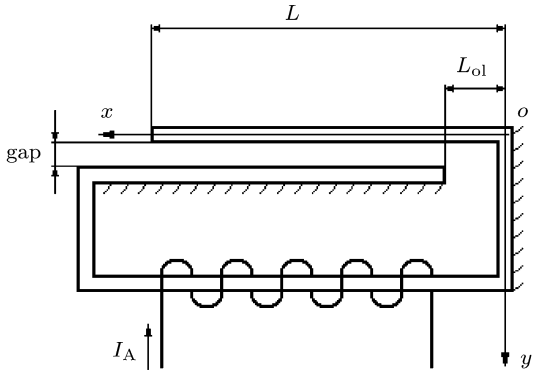


Fig.2. A schematic representation of a magnetic cantilever microbeam.

In Fig.2, neglecting the fringing effect, substituting Eqs.(2) and (3) into Eq.(1), and multiplying each term by a normal mode $\phi_i(x)$, integrating along the beam length and calling upon the orthogonality property[18] of the mode shapes leads to

$$m_i\ddot{q}_i(t) + c_i\dot{q}_i(t) + k_i q_i(t) + EI\int_0^L \phi_i(x)\frac{\partial^4 Y_0(x)}{\partial x^4}\mathrm{d}x = \int_0^L \phi_i(x) f(x,y,t)\mathrm{d}x = \int_{L_{\rm ol}}^L \phi_i(x) f(x,y,t)\mathrm{d}x, \quad \text{for } i = 1, \cdots, N, \tag{4}$$

where $m_i = \int_0^L \rho bh\phi_i^2(x)\mathrm{d}x$ is the generalized mass corresponding to mode i, $k_i = EI\int_0^L \phi_i(x)\dfrac{\partial^4\phi_i(x)}{\partial x^4}\mathrm{d}x$ is the generalized stiffness corresponding to mode i,

$c_i = \int_0^L c\phi_i^2(x)\mathrm{d}x$ is the generalized damp corresponding to mode i. The mechanical-magnetic coupling occurs everywhere along the beam length $[L_{\mathrm{ol}},\ L]$, hence the system forms a distributed problem. An approximation algorithm for the distributed problem is as follows. The magnetic microbeam is discretized equably into a finite number of segments M of localized individual magnetic gap elements, or better, two-port magnetic storage elements. Each magnetic element is parallel to x-axis. Obviously the microbeam model is piecewise uniform. The length of each magnetic element is $\Delta = \dfrac{(L - L_{\mathrm{ol}})}{M}$. The x-coordinates of the two extreme points of the jth element are $x_{j-1} = L_{\mathrm{ol}} + (j-1)\Delta$ and $x_j = L_{\mathrm{ol}} + j\Delta$. Thus the discrete form of Eq.(4) is

$$m_i\ddot{q}_i(t) + c_i\dot{q}_i(t) + k_iq_i(t) + EI\int_0^L \phi_i(x)\frac{\partial^4 Y_0(x)}{\partial x^4}\mathrm{d}x = \sum_{j=1}^{M}\phi_i\left(\frac{x_{j-1}+x_j}{2}\right)f\left(\frac{x_{j-1}+x_j}{2}, \frac{y(x_{j-1})+y(x_j)}{2}\right)\Delta,$$
$$\text{for}\quad i = 1, \cdots, N, \tag{5}$$

where $x = \dfrac{x_{j-1}+x_j}{2}$, $y = \dfrac{1}{2}\left[Y_0(x_{j-1}) + Y_0(x_j) + \sum_{m=1}^{N}\phi_m(x_{j-1})q_m(t) + \sum_{m=1}^{N}\phi_m(x_j)q_m(t)\right]$. The reluctance of the jth element can be written as

$$\begin{aligned}&R_j(q_1(t), q_2(t), \cdots, q_N(t))\\ =&\frac{Mg}{\mu_0 A_{\mathrm{g}}} - \frac{M}{2\mu_0 A_{\mathrm{g}}}\left[Y_0(x_{j-1}) + Y_0(x_j) + \sum_{m=1}^{N}\phi_m(x_{j-1})q_m(t) + \sum_{m=1}^{N}\phi_m(x_j)q_m(t)\right]\\ &\text{for}\quad i = 1, \cdots, N,\end{aligned} \tag{6}$$

where μ_0 is the free-space permeability, A_{g} is the gap area of the magnetic core, $A_{\mathrm{g}} = b(L - L_{\mathrm{ol}})$.

In conventional macroscopic case, the reluctance of the magnetic core is usually negligibly small compared with that of the gap. Thus most of the magnetic energy is stored in the gap. But in microscopic case, the reluctance of the magnetic core has a value comparable to or even exceeds that of the gap.[1,3] The total energy stored in the system is the sum of the energies stored in the core and the gap. Then the total energy can be written as[3]

$$W_{\mathrm{Mag}} = \frac{n^2 I_{\mathrm{A}}^2}{2(R_{\mathrm{core}} + R_{\mathrm{gap}})}, \tag{7}$$

where n is the number of turns of conductor coil in the core length of l_{core}. R_{core} is the reluctance of the magnetic core, which can be written as[1,3]

$$R_{\mathrm{core}} = \frac{l_{\mathrm{core}}}{\mu_0\mu_{\mathrm{r}}A_{\mathrm{c}}} \tag{8}$$

with A_{c} being the cross sectional area of the magnetic core, μ_{r} the relative permeability. In addition, we assume that the magnetic material is magnetically linear. R_{gap} is the reluctance of the gap. It consists of parallel connection of all magnetic element reluctances. Note that Eq.(6) is the reluctance of the jth element, thus R_{gap} can be expressed as

$$R_{\mathrm{gap}} = \left[\sum_{j=1}^{M}\frac{1}{R_j}\right]^{-1}. \tag{9}$$

The magnetic force in the y-direction on the jth element can be expressed as

$$\begin{aligned}&f\left(\frac{x_{j-1}+x_j}{2}, \frac{y(x_{j-1})+y(x_j)}{2}, t\right)\Delta\\ =&\frac{\partial W_{\mathrm{mag}}}{\partial\left(\dfrac{y(x_{j-1})+y(x_j)}{2}\right)}\\ =&\frac{n^2 I_{\mathrm{A}}^2 R_{\mathrm{gap}}^2}{2(R_{\mathrm{core}}+R_{\mathrm{gap}})^2}\frac{M}{\mu_0 A_{\mathrm{g}} R_j^2}.\end{aligned} \tag{10}$$

Note that R_{gap} and R_j are functions of $q_1(t)$, $q_2(t), \cdots, q_N(t)$. Substitution of Eq.(10) into Eq.(5) yields

$$\begin{aligned}&m_i\ddot{q}_i(t) + c_i\dot{q}_i(t) + k_iq_i(t) + EI\int_0^L \phi_i(x)\frac{\partial^4 Y_0(x)}{\partial x^4}\mathrm{d}x\\ =&I_A^2\cdot F_i(q_1(t), q_2(t), \cdots, q_N(t))\\ &\text{for}\quad i = 1, \cdots, N,\end{aligned} \tag{11}$$

where

$$F_i(q_1(t), q_2(t), \cdots, q_N(t)) = \frac{Mn^2R_{\text{gap}}^2}{2\mu_0 A_{\text{g}}(R_{\text{core}}+R_{\text{gap}})^2}\left(\sum_{j=1}^{M}\frac{\phi_i\left(\frac{x_{j-1}+x_j}{2}\right)}{R_j^2}\right).$$

If the number of segments $M \to \infty$, it means that the magnetic microbeam is distributed over an infinite number of localized individual magnetic gap elements, thus $\Delta = \mathrm{d}x$, $\frac{A_{\text{g}}}{M} = b\mathrm{d}x$, $x = \frac{x_{j-1}+x_j}{2}$, $y(x) = \frac{y(x_{j-1})+y(x_j)}{2}$, $R_j(q_1(t), q_2(t), \cdots, q_N(t)) = \frac{g-y(x)}{\mu_0 b\mathrm{d}x}$, $R_{\text{gap}} = \left[\int_{L_{\text{ol}}}^{L}\frac{\mu_0 b\mathrm{d}x}{g-y(x)}\right]^{-1}$.

In conventional macroscopic case, the reluctance of the magnetic core $R_{\text{core}} \approx 0$, Eq.(10) can be rewritten as

$$f(x, y(x), t)\mathrm{d}x = \frac{n^2 I_{\text{A}}^2}{2}\frac{\mu_0 b}{(g-y(x))^2}\mathrm{d}x. \tag{12}$$

Substituting Eq.(12) into Eq.(1), we obtain

$$\rho bh\frac{\partial^2 y}{\partial t^2} + c\frac{\partial y(x,t)}{\partial t} + EI\frac{\partial^4 y}{\partial x^4} = \frac{n^2 I_{\text{A}}^2}{2}\frac{\mu_0 b}{(g-y(x))^2}. \tag{13}$$

Substituting $I_{\text{A}} = I_0 + i(t)$ and $y(x,t) = Y_0(x) + \hat{y}(x,t)$ into Eq.(13), we obtain

$$\rho bh\frac{\partial^2 y}{\partial t^2} + c\frac{\partial y(x,t)}{\partial t} + EI\frac{\partial^4 y}{\partial x^4} = \frac{n^2(I_0+i(t))^2}{2}\frac{\mu_0 b}{(g-(Y_0+\hat{y}(x,t)))^2}. \tag{14}$$

Note that $i(t) \ll I_0$ and $\hat{y}(x,t)$ is a small value, we expand the right side of Eq.(14) in a Taylor series around $[I_0, Y_0(x)]$ up to linear order, and rewrite Eq.(14) as

$$\rho bh\frac{\partial^2 \hat{y}}{\partial t^2} + c\frac{\partial \hat{y}(x,t)}{\partial t} + EI\frac{\partial^4 \hat{y}}{\partial x^4} = \frac{n^2 I_0 \mu_0 b}{(g-Y_0(x))^2}i(t) + \frac{n^2 I_0^2 \mu_0 b}{(g-Y_0(x))^3}\hat{y}(x,t). \tag{15}$$

Equation (15) is the small signal dynamic model for macroscopic magnetic actuator. It is in agreement with the Tilmans' result.[10]

In magnetic micro-electronic mechanical system (MEMS) device, as the reluctance of the magnetic core has a value comparable to or even exceeds the gap reluctance due to the fabrication limitations,[1,3] Eq.(10) can be rewritten as

$$f(x,y,t)\mathrm{d}x = \frac{n^2 I_{\text{A}}^2\left(\left[\int_{L_{\text{ol}}}^{L}\frac{\mu_0 b\mathrm{d}x}{g-y(x)}\right]^{-1}\right)^2}{2\left(R_{\text{core}}+\left[\int_{L_{\text{ol}}}^{L}\frac{\mu_0 b\mathrm{d}x}{g-y(x)}\right]^{-1}\right)^2}\frac{\mu_0 b\mathrm{d}x}{(g-y(x))^2}. \tag{16}$$

Substituting Eq.(16) into Eq.(1), we obtain

$$\rho bh\frac{\partial^2 y}{\partial t^2} + c\frac{\partial y(x,t)}{\partial t} + EI\frac{\partial^4 y}{\partial x^4} = \frac{n^2 I_{\text{A}}^2}{2\left(R_{\text{core}}\int_{L_{\text{ol}}}^{L}\frac{\mu_0 b\mathrm{d}x}{g-y(x)}+1\right)^2}\frac{\mu_0 b}{(g-y(x))^2}. \tag{17}$$

Substituting $I_{\text{A}} = I_0 + i(t)$ and $y(x,t) = Y_0(x) + \hat{y}(x,t)$ into Eq.(17), and expanding the right side of the equation in a Taylor series around $[I_0, Y_0(x)]$ up to linear order, we obtain

$$\rho bh\frac{\partial^2 \hat{y}}{\partial t^2} + c\frac{\partial \hat{y}}{\partial t} + EI\frac{\partial^4 \hat{y}}{\partial x^4} = \frac{n^2 I_0}{\left(R_{\text{core}}\int_{L_{\text{ol}}}^{L}\frac{\mu_0 b\mathrm{d}x}{g-Y_0(x)}+1\right)^2}\frac{\mu_0 b}{(g-Y_0(x))^2}i(t) + \left[\frac{1}{\left(R_{\text{core}}\int_{L_{\text{ol}}}^{L}\frac{\mu_0 b\mathrm{d}x}{g-Y_0(x)}+1\right)^2}\frac{n^2 I_0^2 \mu_0 b}{(g-Y_0(x))^3} - \frac{n^2 I_0^2 R_{\text{core}}\int_{L_{\text{ol}}}^{L}\frac{\mu_0 b\mathrm{d}x}{(g-Y_0(x))^2}}{\left(R_{\text{core}}\int_{L_{\text{ol}}}^{L}\frac{\mu_0 b\mathrm{d}x}{g-Y_0(x)}+1\right)^3}\frac{\mu_0 b}{(g-Y_0(x))^2}\right]\hat{y}. \tag{18}$$

This equation is the small signal dynamic model for magnetic flexible microbeam.

3. Example

3.1. Static deflection of a magnetic microbeam actuator

In order to validate the model in this paper, the static deflection of a cantilever microbeam actuator[1] with a multilever meander magnetic core is calculated as a function of the dc coil current varying from 0.2 to 0.9A. The geometrical and magnetic parameters[1] of this actuator are listed in Table 1. The initial deflection of the microbeam $Y_0(x)$ equals zero. Considering $L \gg g$, the linear mode functions of cantilever beam at $Y_0(x)$=0 are used as basis functions. To calculate the static deflection of the microbeam, the time derivatives and the ac current are set to zero in Eq.(11). Thus it can be rewritten as

$$k_i q_i = I_0^2 F_i(q_1, q_2, \cdots, q_N) \quad \text{for} \quad i = 1, \cdots, N, \quad (19)$$

where

$$F_i(q_1, q_2, \cdots, q_N) = \frac{M n^2 R_{\text{gap}}^2}{2\mu_0 A_{\text{g}} (R_{\text{core}} + R_{\text{gap}})^2} \left(\sum_{j=1}^{M} \frac{\phi_i\left(\dfrac{x_{j-1} + x_j}{2}\right)}{R_j^2} \right),$$

$q_1, q_2, \cdots, q_N$ are N unknown quantities. Self-consistent method[12] is used to solve the N nonlinear coupling equations. The microbeam deflection curve is described as

$$y(x) = \sum_{m=1}^{N} \phi_m(x) q_m = I_0^2 \left[\sum_{m=1}^{N} \frac{F_m(q_1, q_2, \cdots, q_N)}{k_m} \phi_m(x) \right]. \quad (20)$$

Table 1. The parameters of a magnetic micro-actuator.[1]

parameters/units	value
gap g/μm	10
beam width b/μm	25
beam thick h/μm	2.5
beam length L/μm	780
overlap length $(L - L_{\text{ol}})/\mu$m	770
young's modulus E/Pa	2.06×10^8
coil turns n	17
core length l_{core}/μm	2400
space permeability μ_0/(H/m)	$4\pi\times10^{-7}$
relative permeability μ_{r}	500

Figure 3 shows a plot of the cantilever microbeam tip ($x = L$) displacement obtained by solving Eq.(19) and calculating Eq.(20) for various values of current I_0 using the first one-, two mode discretizations and five-, ten integration segments, where N is the number of selected modes, M is the number of integration segments. For comparison, the experimental results available in Ref.[1] for the cantilever microbeam tip ($x = L$) displacement is also plotted in Fig.3. In fact, in order to check how many modes should be kept, we also used the first three modes to calculate the tip displacement. We found that the results of the three modes are almost the same as the results of the first two modes. Thus, we adopt only the first two terms of Eqs.(3) and (19), the results of the three modes are not plotted in Fig.3.

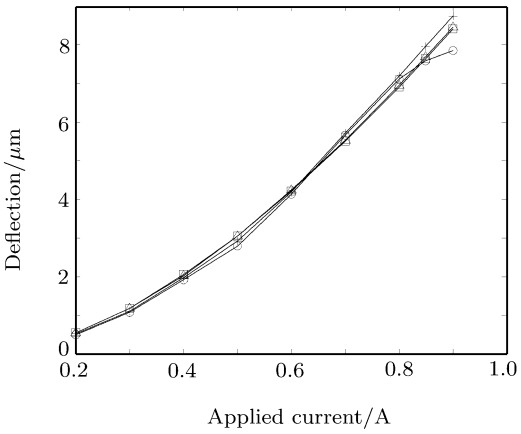


Fig.3. Comparison of the microbeam tip deflections calculated by the present model and obtained by experiment.[1] Solid line with circles—Experimental results;[1] Solid line with squares—N=1, M=5; Solid line with triangles—N=1, M=10; Solid line with pluses—N=2, M=10.

In Fig.3, it can be seen that for small currents and displacements, there is good agreement among all the four lines. When the displacement approaches about 5μm, there is also good agreement between the solid line with triangles and the solid line with squares, but the solid line with pluses departs from the solid line with triangles and the solid line with squares. These results suggest that the number of selected modes N has more effect to the calculation results than the number of integration segments M. Because the microbeam deflection is less than 10μm (gap separation), it is very small relative to the microbeam length (780μm). So the microbeam deflection curve is nearly a straight line, the number of integration segments M has almost no effect on the calculation results. Now we compare our results with experimental results.[1] We observe that the solid line with triangles, the solid line with squares, and the solid line with pluses are

all in good agreement with experiment results (solid line with circles) while the dc current I_0 is less than 0.8A, but the solid line with pluses is clearly more accuracy than those with triangles and the squares. When the dc current I_0 exceeds 0.8A, the deflection begins to saturate, which is caused by the magnetic flux saturation in the magnetic core.

3.2. Magnetic force acting on microbeam

Note that Eq.(10) is the magnetic force in the y-direction on the jth element, so the magnetic total force acting on the microbeam can be expressed as

$$\begin{aligned} P =& \sum_{j=1}^{M} f\left(\frac{x_{j-1}+x_j}{2}, \frac{y(x_{j-1})+y(x_j)}{2}, t\right)\Delta \\ =& I_0^2\left[\sum_{j=1}^{M}\frac{n^2R_{\rm gap}^2}{2(R_{\rm core}+R_{\rm gap})^2}\right. \\ & \left.\times\frac{M}{\mu_0 A_{\rm g}R_j^2(q_1,q_2,\cdots,q_N)}\right]. \end{aligned} \tag{21}$$

In order to validate the accuracy of Eq.(19), the magnetic total force acting on the microbeam is also calculated using an approximation algorithm.[3] This algorithm is based on the derivative of the magnetic energy. The main steps of the approximation algorithm are summarized as follows: Firstly, the deflection curve of microbeam is assumed to be a straight line, and the experimental results available in Ref.[1] for the cantilever microbeam tip ($x = L$) displacements are used as the cantilever microbeam tip displacements $y(L)$ for various values of dc current I_0. Secondly, finite element simulators (ANSYS) are used in two times the first time it set to obtain magnetic energy; with the deflection of the cantilever microbeam position as 0, and the second time is set the deflection of the cantilever microbeam position as $y(L)$. The magnetic force is then determined

$$F = \frac{\partial W(y(L))}{\partial y(L)} \approx \frac{W(y(L))-W(0)}{y(L)}, \tag{22}$$

where $W(0)$ and $W(y(L))$ are the magnetic energy of the microbeam actuator system at position 0 and $y(L)$, respectively.

Figure 4 shows the curves of the total magnetic force acting on the cantilever microbeam obtained by employing the approximation algorithm equation (22) and by solving Eqs.(19)–(21) using one/two mode discretizations and five/ten integration segments, respectively. It is clear in Fig.4 that for small currents and displacements, there is good agreement among all four curves. However, for large currents and displacements, the solid line with pluses and the solid line with circles are still very close to each other, the solid line with triangles and the solid line with squares are still very close but depart from the solid lines with circles and pluses. This means that the number of selected modes N has more effect on the calculation results than the number of integration segments M, and that the solid line with pluses is clearly more accurate than the solid line with triangles and the solid line. The reason for this has already been mentioned before. It should be stressed that the nonlinear property between magnetic induction B and magnetic field intensity H has been neglected in ANSYS, so the magnetic flux saturation in the magnetic core is disappearance.

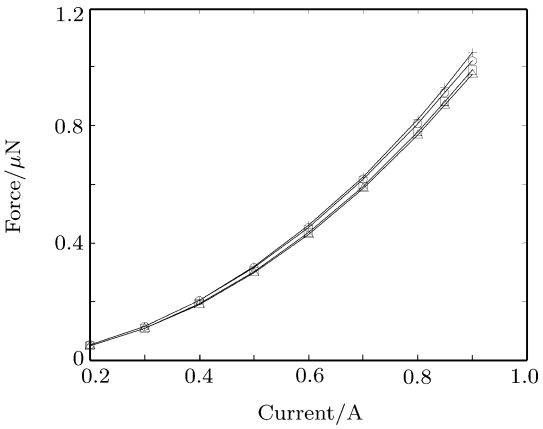


Fig.4. Comparison of the total magnetic forces acting on the cantilever microbeam calculated by the present model and by an approximation algorithm.[3] Solid line with circles—An approximation algorithm;[3] Solid line with triangles—N=1, M=5; Solid line with squares—N=1, M=10; Solid line with pluses—N=2, M=10.

3.3. Transient response of the microbeam

Now the transient behaviour of the microbeam around its statically deflected position will be analysed. For comparison, two statically deflected positions, corresponding to the dc polarization currents I_0=0.2A and I_0=0.8A, are selected. The ac component $i(t)$ is an impulse function. Using Eq.(18), the

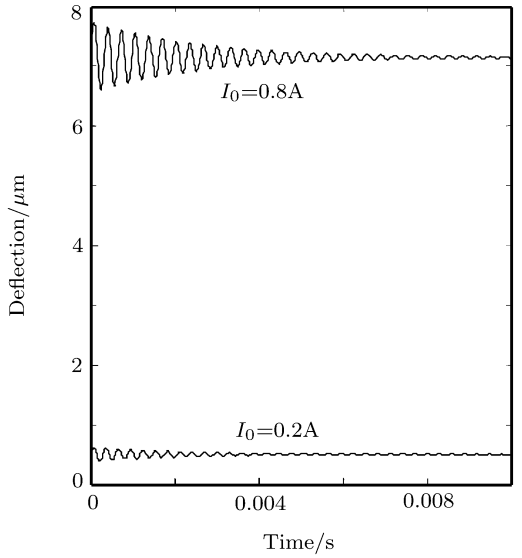


Fig.5. Comparison of the two impulse responses of the microbeam at 0.8A and 0.2A.

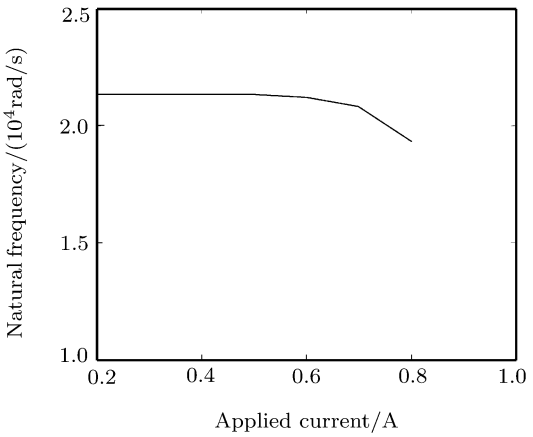


Fig.6. The natural frequency changes as a function of the dc current.

microbeam responses (tip deflections) to the two statically deflected positions are calculated as functions of time. Figure 5 shows the comparison of the two responses. It can be seen that the amplitude of response at I_0=0.8A is larger than that at I_0=0.2A, and the natural frequency at I_0=0.8A is smaller than that at I_0=0.2A. It means that increasing the dc bias current weakens the microbeam stiffness, shifts the natural frequency to small values of it. Figure 6 shows the characteristic, which is similar to electrostatic actuator: increasing the electrostatic force shifts the natural frequency to small values of it.

4. Conclusions

A mechanic-magnetic coupling macroscopic model for a magnetic microbeam actuator has been presented using the linear mode shapes of a microbeam as basis functions. In comparison with previous models, the present model can account for the micro-magnetic-core reluctance and the coupling between the beam deflection and the magnetic force. It has been validated by comparing its results with experimental ones available in the related papers and finite-element solutions. The example given in this paper also shows that using the linear mode shapes of a microbeam as basis functions can yields enough accuracy for small deflections. The number of integration segments M has almost no effect on the calculation results because the microbeam deflection curve is nearly a straight line in the small deflection case.

References

[1] Ahn C H and Allen M G 1993 *IEEE J. Microelectromech. Syst.* **1** 15
[2] Judy J W and Muller R S 1995 *IEEE J. Microelectromech. Syst.* **4** 162
[3] Nami Z, Ahn C H and Allen M G 1996 *J. Micromech. Microeng.* **3** 337
[4] Judy J W and Muller R S 1996 *Sensors and Actuators* A **53** 392
[5] Lagure L K and Brand O 1999 *IEEE J. Microelectromech. Syst.* **1** 2
[6] Ludwig A and Quandt E 2000 *J. Appl. Phys.* **9** 4691
[7] Chin T S 2000 *J. Magn. Magn. Mater.* **209** 75
[8] Niarchos D 2003 *Sensors and Actuators* A **106** 255
[9] Tilmans H A C 1996 *J. Micromech. Microeng.* **7** 157
[10] Tilmans H A C 1996 *J. Micromech. Microeng.* **7** 285
[11] Aluru N R and White J 1997 *Sensors and Actuators* A **58** 1
[12] Aluru N R and White J 1999 *IEEE J. Microelectromech. Syst.* **3** 299
[13] Li G and Aluru N R 2001 *Sensors and Actuators* A **91** 278
[14] Younis M I, Abdel-Rahman E M and Nayfeh A 2003 *IEEE J. Microelectromech. Syst.* **5** 672
[15] Abdel-Rahman E M, Younis M I and Nayfeh A 2003 *J. Micromech. Microeng.* **12** 759
[16] Yu X M, Zhang D C, Wang C S, Li T and Ruan Y 2004 *Acta Phys. Sin.* **53** 31 (in Chinese)
[17] Chen D P, Dong F L, Guo Z Y, Li C B, Mou Z Y, Wu X P, Xiong Z M and Zhang Q C 2007 *Acta Phys. Sin.* **56** 2529 (in Chinese)
[18] Meirovitch L 1975 *Elements of Vibration Analysis* (New York: McGraw-Hill)